Available online at www.springerlink.com

Acta Metall. Sin. (Engl. Lett.) Vol.26 No. 5 pp. 545—552 October 2013

ACTA
METALLURGICA SINICA
(ENGLISH LETTERS)

Assessment of Sensitization in AISI 304 Stainless Steel by Nonlinear Ultrasonic Method

Saju T. Abraham[1)†], *S.K. Albert*[1)], *C.R. Das*[1)], *N. Parvathavarthini*[1)], *B. Venkatraman*[1)], *R.S. Mini*[2)] *and K. Balasubramaniam*[3)]

1) Quality Assurance Division, Indira Gandhi Centre for Atomic Research, Kalpakkam 603 102, India
2) Department of Mechanical Engineering, Government Engineering College, Thiruvananthapuram-695035, India
3) Department of Mechanical Engineering, Indian Institute of Technology, Madras Channai 600 036, India

[Manuscript received 26 March 2013, in revised form 18 June 2013]

A nonlinear ultrasonic technique has been developed to evaluate sensitization in Type 304 stainless steel. In order to achieve different degree of sensitization (DOS), specimens have been subjected to heat treatment at 675 °C at varying soaking time (0.5, 1.0, 2.0, 3.0 and 4.0 h). Heat treated specimens were subjected to intergranular corrosion tests as per ASTM standards A262 and G108. Sensitization in longer soaked material has been confirmed through ditch microstructures, cracks on the bend tested specimens and higher degree of sensitization. Nonlinear ultrasonic studies showed variation in the nonlinearity parameter with soaking time which also confirms sensitization. A good correlation was observed between the degree of sensitization measured by the electrochemical potentiokinetic reactivation test and the ultrasonic nonlinearity parameter. This study clearly demonstrated that nonlinear ultrasonic technique can be used as a potential technique for non-destructive characterization of sensitization in austenitic stainless steel.

KEY WORDS: Austenitic stainless steel; Degree of sensitization; Intergranular corrosion; Nonlinear ultrasonics

1. Introduction

Austenitic stainless steel has wide applications at higher temperatures for its good mechanical properties, corrosion resistance, formabilities and weldabilities [1]. These superior properties make the austenitic stainless steel to be widely used in nuclear industry. However, heat treatment of this steels for a sufficiently long time in the range from 450 °C to 800 °C leads to formation of chromium carbide ($Cr_{23}C_6$) precipitate along the prior austenite grain boundaries resulting depletion of chromium in the vicinity of the boundaries which make this material susceptible to inter granular corrosion (IGC). This phenomenon is called sensitization[2−6]. Susceptibility to inter granular corrosion can be qualitatively evaluated by different practices described in ASTM (American Society for Testing and Materials) standard A262. On the other hand, the degree of sensitization (DOS) can be evaluated quantitatively by means of electrochemical potentiokinetic reactivation (EPR) test as per the ASTM standard G108. EPR technique is nondestructive, quantitative and rapid for detecting sensitization in austenitic stainless steels[7]. However, application of these techniques is limited within the laboratory. EPR test is strongly dependent on the testing temperature and reveals only the surface features and also the EPR parameters have to be carefully interpreted in the presence of sulphide inclusions[8].

Detection of sensitization is important for safe and reliable operation of a plant. Numerous failures of austenitic stainless steel components caused by IGC have been reported[9,10]. Therefore, characterization of sensitization or IGC is an important aspect for remnant life assessment. Nondestructive evaluation (NDE) techniques play an important role in life assessment of components. Eddy current based nondestructive testing was applied to austenitic stainless steel weldments to assess and quantify degree of

† Corresponding author. Tel.: +91 44 27 480 071, Fax: +91 44 27 480 209; E-mail address: sajuta@igcar.gov.in; at.saju@gmail.com (Saju T. Abraham)

DOI: 10.1007/s40195-013-0168-y

sensitization[11,12]. Presence of defects, wall thickness variations, change in permeability and conductivity and surface roughness affect eddy current testing. Also eddy current testing is a subsurface test method. On the other hand, ultrasonic testing, being one of the most widely used NDE techniques for the evaluation of materials which relay on measuring the reflected sound waves, is influence by defect size. Size of the precipitates in the sensitized material is significantly smaller than the wavelength of ultrasonic waves used in NDE and this limits the application of conventional ultrasonic technique to be used in the evaluation of sensitization. An attempt has been made on detection of sensitization in AISI 304 SS by ultrasonic spectrum analysis and attenuation studies[13]. But this method was not effective in quantifying the degree of sensitization. To overcome these limitations in the conventional NDE methods, nonlinear ultrasonic (NLU) technique, using the higher harmonic analysis, is found to be effective. Nonlinear ultrasonics generally involves the investigation of acoustic harmonics generated from the nonlinear interactions of the initially pure sinusoidal ultrasonic waves with lattice anharmonicity of the materials, microstructures of solids, defects, boundaries in crystal structure *etc.* In reality, no solid is perfectly homogenous. When a pure sinusoidal ultrasonic wave of sufficient energy propagates through a solid martial, the lattice anharmonicity present in the material causes distortions in the wave so that higher harmonics of the fundamental frequency will be generated as shown schematically in Fig. 1.

The dependence of the acoustic nonlinearity parameters on the crystalline structure suggests that the geometry of the local atomic arrangement and shape, rather than the strength of the interatomic potential are dominant factors in determining the magnitude of the nonlinearity parameter[14]. Material defects and microstructure can significantly alter the crystal structure or symmetry which could lead to changes in the values of the nonlinear ultrasonic parameters. NLU technique has been widely used for characterization of precipitation hardening[15], microstructure[16], dislocations[17] *etc.* It is also sensitive to ageing[18], creep[19,20], cold work[21], fatigue[22−28], cracks[29], radiation damage[30] and thermal degradation[31,32]. Objective of the present study is to evaluate sensitization in AISI 304 stainless steel using nonlinear ultrasonic technique.

2. Ultrasonic Nonlinearity Parameter

The linear relation between stress (σ) and strain (ε) for an elastic solid is given by the Hooke′s law

$$\sigma = E\varepsilon \tag{1}$$

This linear relation has been derived on the assumption of infinitesimal amplitude of the elastic waves propagating in the homogeneous material and

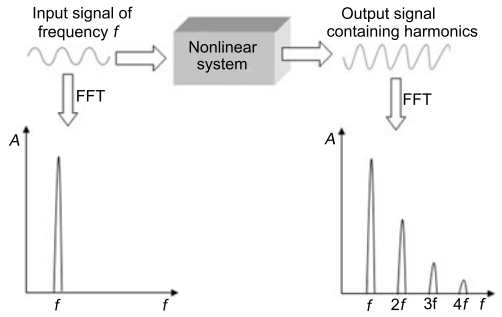

Fig. 1 Schematic diagram of the harmonic generation in a nonlinear solid and the corresponding frequency spectra

is applicable only for ideal linear elastic media that does not exist in nature. This linear law is valid for a homogenous and isotropic medium when the applied stress amplitude is infinitesimal. However, materials in nature are not perfectly homogeneous and isotropic and hence the stress-strain relationship can be expressed by the power series expansion of strain as

$$\sigma = E_1\varepsilon + \frac{1}{2}E_2\varepsilon^2 \tag{2}$$

where, $\varepsilon = \frac{\partial u}{\partial x}$ is the strain, σ is the stress, E_1 and E_2 are the elastic coefficients.

Consider the one dimensional wave equation

$$\rho\frac{\partial^2 u}{\partial t^2} = \frac{\partial \sigma}{\partial x} \tag{3}$$

Substituting Eq. (2) in Eq. (3), we get

$$\rho\frac{\partial^2 u}{\partial t^2} = E_1\frac{\partial^2 u}{\partial x^2} + E_2\frac{\partial}{\partial x}\frac{\partial^2 u}{\partial x^2} \tag{4}$$

An approximate solution to Eq. (4) can be found through the use of perturbation theory where the displacement (u) is assumed to be of the form

$$u = u_0 + u_1 \tag{5}$$

It is also assumed that

$$E_1 >> E_2, \text{ and } u_0 >> u_1$$

Substituting Eq. (5) into Eq. (4),

$$\rho\frac{\partial^2(u_0+u_1)}{\partial t^2} = E_1\frac{\partial^2(u_0+u_1)}{\partial x^2} + E_2\frac{\partial(u_0+u_1)}{\partial x}\frac{\partial^2(u_0+u_1)}{\partial x^2} \tag{6}$$

When this equation is expanded and rearranged by considering the linear solution

$$\rho\frac{\partial^2 u_0}{\partial t^2} = E_1\frac{\partial^2 u_0}{\partial x^2}$$

and the perturbation conditions given above, we get

$$\rho\frac{\partial^2 u_1}{\partial t^2} = E_1\frac{\partial^2 u_1}{\partial x^2} + E_2\frac{\partial u_0}{\partial x}\frac{\partial^2 u_0}{\partial x^2} \tag{7}$$

Table 1 Chemical composition (wt.%) of the experimental steel

C	Mn	Si	S	P	Cr	Ni	Mo	Ti
0.053	0.803	0.494	0.021	0.054	18.356	10.498	0.308	0.011
Cu	Nb	Al	V	B	Co	Sn	Pb	N
0.045	0.010	0.001	0.008	0.0003	0.081	0.007	0.000	0.024

Table 2 Parameters of heat treatment of the experimental steel

Specimen No.	Heat rate (°C/h)	Soaking temperature (°C)	Soaking time (h)
1	200	675	0.5
2	200	675	1.0
3	200	675	2.0
4	200	675	3.0
5	200	675	4.0

A solution to this first order equation can be found as

$$u_0 = A_1 \sin(\omega t - kx) \tag{8}$$

Substituting Eq. (8) into Eq. (7),

$$\rho \frac{\partial^2 \mu_1}{\partial t^2} = E_1 \frac{\partial^2 u_1}{\partial x^2} - \frac{1}{2} E_2 A_1^2 k^3 \sin 2(\omega t - kx) \tag{9}$$

It is to be noted that the second term in Eq. (9) is a second harmonic sinusoid. One solution to u_1 in Eq. (9) is

$$u_1 = -\frac{1}{8}\Big(\frac{E_2}{E_1}\Big) k^2 A_1^2 x \cos 2(\omega t - kx) \tag{10}$$

This solution indicates that the amplitude of the perturbation (second harmonic) is

$$|A_2| = \frac{1}{8}\Big(\frac{E_2}{E_1}\Big) k^2 A_1^2 x \tag{11}$$

occurring at frequency of 2ω. The nonlinearity parameter β is then defined from Eq. (11) as

$$\beta = \frac{E_2}{E_1} = \frac{8}{k^2 x} \frac{A_2}{A_1^2} \tag{12}$$

where A_1 is the amplitude of the fundamental wave, A_2 is the amplitude of the second harmonic wave, k is the wave number and x is the propagation distance. This equation implies that the nonlinearity parameter β of a material can be evaluated by measuring the absolute amplitudes of the fundamental and second harmonic components and can be correlated to the changes responsible for the nonlinear behavior.

3. Experimental

3.1 Specimen preparation

Solution annealed AISI 304 stainless steel plate of 12 mm thickness was chosen as the material of interest in this work. Chemical composition of this steel was analyzed by optical emission spectroscopy as per the ASTM standard E1086 and was given in Table 1. The plate was cut into a number of pieces for different experiments and grouped them into five sets. Each set has been subjected to sensitization heat treatment in a muffle furnace. In order to obtain different degree of sensitization in these specimen blanks, heat treatments were carried out at 675 °C for 0.5, 1.0, 2.0, 3.0 and 4.0 h as given in Table 2. Temperature variation at the test temperature was ±1 °C. After completion of heat treatment, specimens were cooled inside the furnace. These specimens were then subjected to intergranular corrosion tests such as oxalic acid etch test, bend test, electrochemical potentiokinetic reactivation test followed by nonlinear ultrasonic testing.

3.2 Intergranular corrosion tests

3.2.1 Oxalic acid etch test

For performing the oxalic acid etch test as per the ASTM standard A262 practice A, a 10 mm×10 mm sample was cut from every heat treated specimens. These samples were mounted in epoxy resin and polished up to the diamond finish. The polished specimens were electrolytically etched for 90 s in 10 wt.% oxalic acid solution and then examined under optical microscope.

3.2.2 Bend test

To determine the susceptibility to intergranular attack associated with the precipitation of chromium rich carbides around the grain boundaries, Cu-$CuSO_4$-16% H_2SO_4 test as per practice E was conducted on the specimens. This test involves exposure of heat treated specimens in this solution followed by 180 °C bending. Degree of sensitization is qualitatively revealed by the extent of crack appeared on the convex surface.

3.2.3 Electrochemical potentiokinetic reactiva-tion (EPR) test

The intergranular corrosion resistance was examined by double loop electrochemical potentiokinetic reactivation (EPR) test following ASTM standard G108. For each specimen, the activation and reactivation curves are recorded. From these curves, degree of sensitization (DOS) was evaluated by Eq. (13)

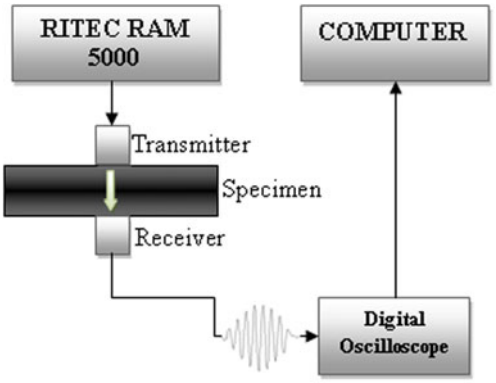

Fig. 2 Schematic diagram of the experimental setup for nonlinear ultrasonics

$$DOS = \frac{I_{\mathrm{r}}}{I_{\mathrm{a}}} \times 100\% \tag{13}$$

where, I_{r} is the reactivation current density and I_{a} is the activation current density. Lower the DOS higher the corrosion resistance.

3.3 Nonlinear ultrasonic testing

Second harmonic generation technique was used to measure the ultrasonic nonlinearity parameter of the heat treated specimens. Schematic of the experimental set up is shown in Fig. 2. Two ultrasonic transducers are placed on either side of the specimen to transmit and receive the signal. The specimens were polished with 600 g emery paper to obtain proper coupling with the ultrasonic transducers. In order to maintain alignment and parallelism between the two transducers and to fix them properly on the surface of the material with proper contact and constant pressure, a special fixture was designed. Non-viscous oil was used as the coupling medium. A high power pulser-receiver (RITEC RAM-5000), which is specifically designed for nonlinear ultrasonic measurements, was used for exciting the ultrasonic transducer. Hanning windowed tone burst was excited by a contact longitudinal piezoelectric transducer nominal frequency 5 MHz and diameter 9 mm. Hanning window was selected due to its little effect on the measured nonlinearity[33]. Number of cycles in the tone burst was limited to 10. A long signal improves the accuracy of the measurements but if the signal is too long, the incident and reflected wave interfere at the receiver side. Therefore the signal length was restricted to be slightly lesser than twice the thickness of the material. A broadband 10 MHz transducer was used to acquire the second harmonic waves. The output from the 10 MHz transducer was fed to a digital storage oscilloscope (Agilent 6032A) and the time domain data was stored as CSV format with 1000 data points for post-processing. Amplitudes of the fundamental (A_1) and second harmonic (A_2) waves were obtained by digital signal processing using a fast Fourier transform (FFT).

To increase the accuracy and repeatability, signals have been acquired with different power levels (40% to 100% of RITEC power levels) on each specimen and repeated for different locations on those specimens. A graphical plot is made between A_2 and A_1^2 for the seven different power levels for each specimen and the slope of this graph provides the ultrasonic nonlinearity parameter β. From the obtained β values, a relative β parameter was defined as

$$\beta_{\mathrm{reltive}} = \frac{\beta_{\mathrm{heat\ treated}}}{\beta_{\mathrm{base\ metal}}} \tag{14}$$

4. Results and Discussion

4.1 IGC tests

Optical micrographs of etched specimens are shown in Fig. 3. From Fig. 3(a) it is evident that the base metal has step structure. With 30 min of soaking at 675 °C, the microstructure has become dual, as shown in Fig. 3(b), which indicates that the sensitization is initiated. With further increase in soaking time, ditch structure is formed since the carbides are fully dissolved in electrolytic etching, as shown in Fig. 3(c)—Fig. 3(f), which indicates that the material is fully sensitized after 30 min of soaking.

Photographs of the bend tested specimens as per the practice E are shown in Fig. 4. Exposure of stainless steel to the Cu-$CuSO_4$-16%H_2SO_4 solution led to dissolution of Cr depleted regions. This occurs when there is a total loss of local passivity in these regions as a result of decrease of Cr below 12% which lead to formation of microscopic grooves which acted as stress concentration sites during bend testing. Intergranular cracks are evident in 30 min soaked specimen, Fig. 4(a), indicating the material is susceptible to IGC. With further progress of soaking, severity of IGC cracking increased which resulted peel-off of material from the surface of bend tested specimens, Fig. 4(b)—Fig. 4(e). These photographs clearly indicate that all specimens soaked 30 min and beyond are highly susceptible to IGC.

From the double loop EPR test, the activation and reactivation curves are evident and typical plots for base material and 4.0 h soaked specimens are shown in Fig. 5. From these curves the degree of sensitization is calculated as per the Eq. (13) and is plotted in Fig. 6 as a function of soaking time. DOS value was found to be 0.14% for the base material and this value progressively increased to 10.34, 37.87, 40.30, 37.75 and 38.70 for 0.5 to 4.0 h soaking respectively. Though, maximum DOS was found in 2.0 h soaked specimen, it is clearly evident that DOS value remains constant with marginal variation from 1.0 to 4.0 h soaking. However, for sensitisation experiment, specimens to be heat treated at 675 °C for 1.0 h as per ASTM A262. Therefore, results obtained in the present study are in line with standard practice. Though, DOS value

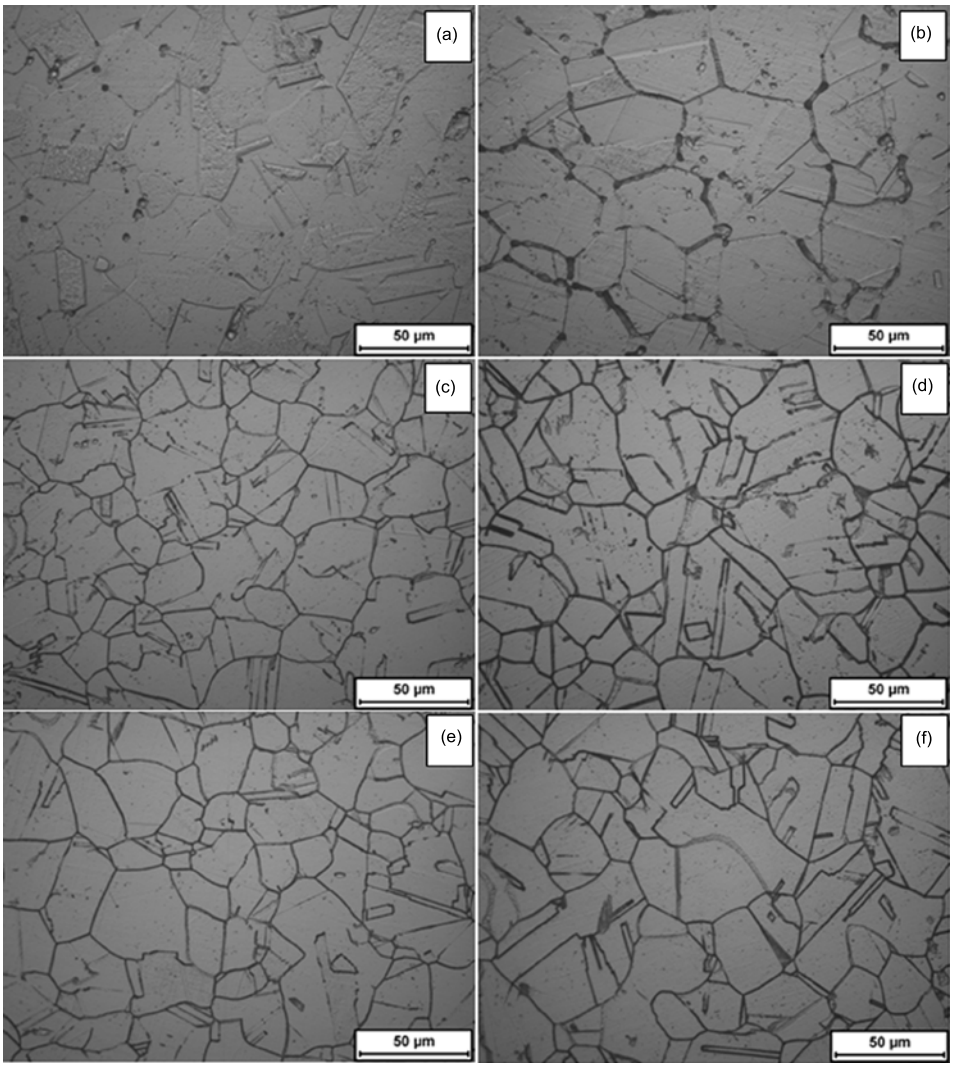

Fig. 3 Typical optical metallographic images of the specimen with different soaking time: (a) base metal showing step structure, (b) 0.5 h showing partial sensitization, (c) 1.0 h, (d) 2.0 h, (e) 3.0 h, (f) 4.0 h showing fully sensitized structure

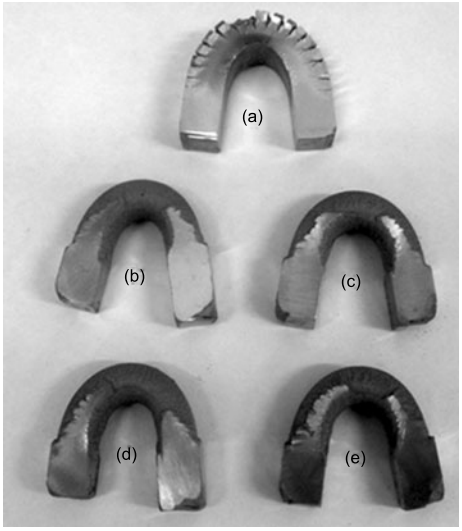

Fig. 4 Specimens after practice-E bend test with different soaking time of 0.5 h (a), 1.0 h (b), 2.0 h (c), 3.0 h (d) and 4.0 h (e)

decreased at 4.0 h soaking (38.70%) from maximum value (40.30%), the change is minimal and hence it can be assumed that 4.0 h is insignificant for any self healing of the sensitized material. Further, study may be required to understand the hold time effect on self-healing.

4.2 NLU test

The fundamental and second harmonic signal amplitudes A_1 and A_2 have been measured for seven different power levels (40 to 100 of RITEC) on each specimen. Fig. 7 shows a particular Hanning windowed signal at these power levels and the respective Fast Fourier Transform spectrum. It is obvious that as the power level increases, amplitude increases.

A typical plot of A_2 *vs.* A_1^2 as a function of increasing power levels is given in Fig. 8 which shows the linear relationship between A_2 and A_1^2 as in Eq. (12). The relative β parameter was calculated from the

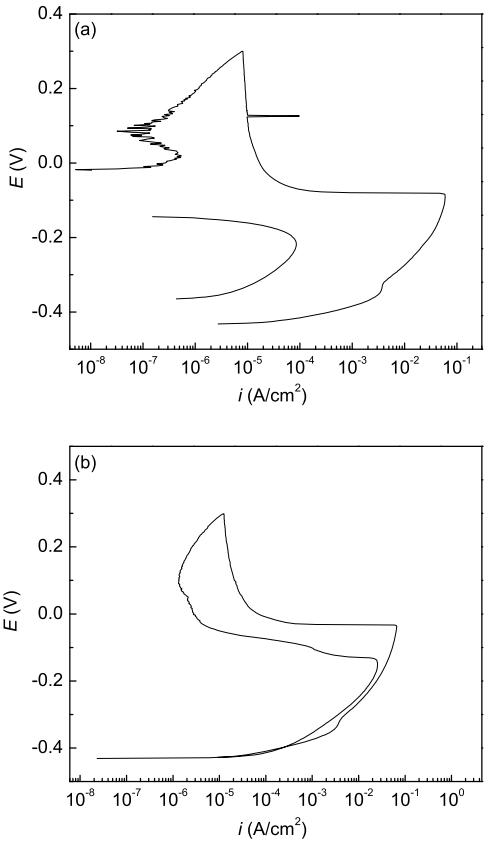

Fig. 5 Activation-reactivation curves for base metal (a) and sensitized specimen with 4.0 h soaking (b)

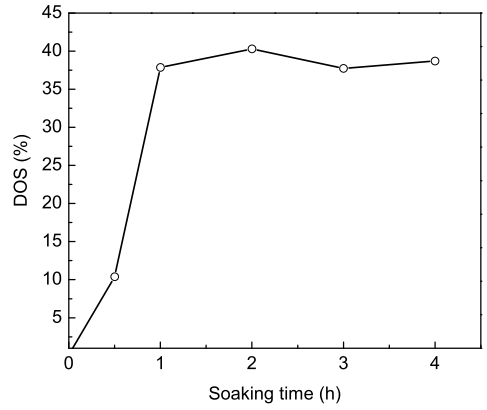

Fig. 6 Curve of degree of sensitization (DOS) *vs.* soaking time

slope of this plot and averaged over the results for a number of experiments. Fig. 9 shows the variation of the relative β (averaged over a number of experiments) with soaking time. For 0.5, 1.0, 2.0, 3.0 and 4.0 h heat treatments β increased by 15%, 40%, 56%, 62% and 63% respectively compared to the base material.

Second harmonic generation is due to the distortion to the sinusoidal form of the ultrasonic waves during propagation in the anharmonic solid. Supported by literatures [2–6] and from the above experimental evidences, it is seen that the dominant microstructural change that leads to the anharmonic behavior in the present study, is the precipitation of chromium carbide along the grain boundaries. Generally, crystal structure of precipitate phase is different from that of the matrix phase. The misfit parameter δ is defined as

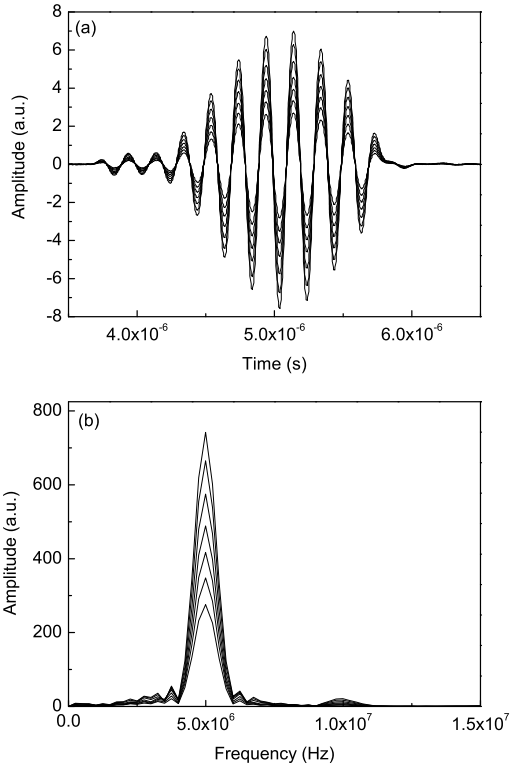

Fig. 7 Signals at seven different power levels: (a) time domain signal, (b) corresponding FFT spectrum

$$\delta = \frac{a_{\mathrm{p}} - a_{\mathrm{m}}}{a_{\mathrm{m}}} \tag{15}$$

where a_{p} is the lattice parameter of the precipitate and a_{m} is the lattice parameter of the matrix. For the fcc austenitic stainless steel matrix, the lattice parameter is 0.359 nm and for the chromium carbide ($Cr_{23}C_6$) precipitate, the lattice parameter is 1.05 nm[1]. This mismatch between the precipitate phase and the matrix produces local strain fields and may increase the stress. The radial stress σ_{r} in the matrix at a radius r from a spherical precipitate of radius r_1 embedded in a finite body matrix is given by[14]

$$\sigma_1 = -\frac{4\mu\delta r_1^3}{r^3} \tag{16}$$

where, δ is the precipitate-matrix lattice misfit parameter and μ is the shear modulus. Hence the local strain fields from the lattice mismatch will increase the stress and at some point of time it is enough to distort the ultrasonic waves to generate higher harmonic components. The increase in β with increase in soaking time is in agreement with the published literature where it was shown that nonlinearity parameter increased from minima value with precipitate

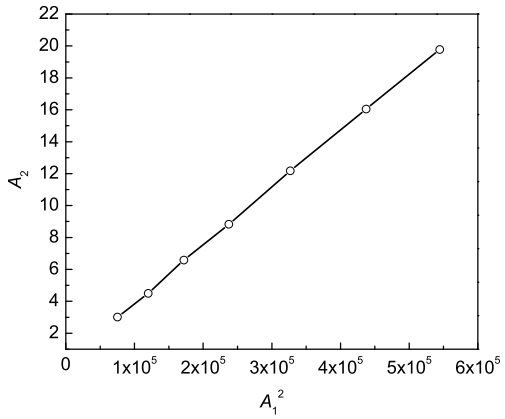

Fig. 8 Variation of A_2 and A_1^2 with increase in power level

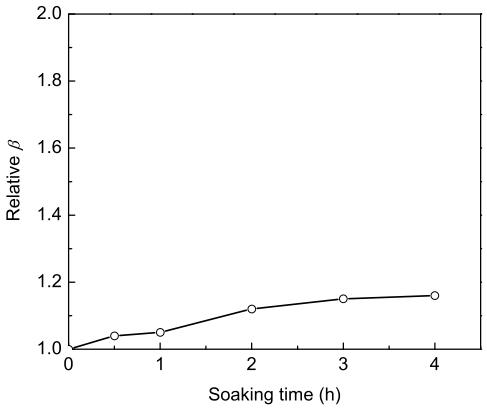

Fig. 10 Variation of relative β of the solution annealed specimens with soaking time

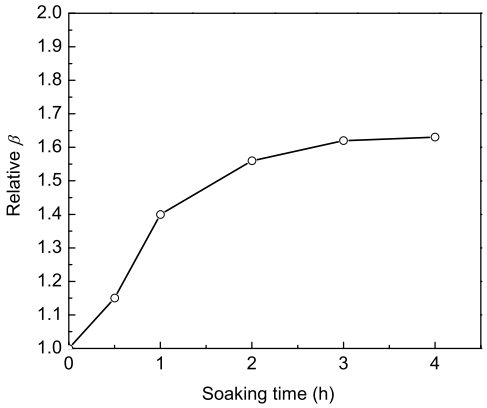

Fig. 9 Variation of relative β of the sensitized specimens with soaking time

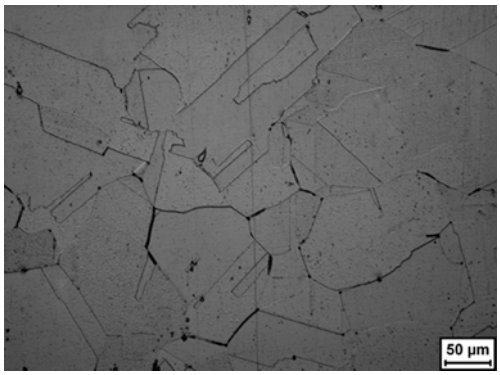

Fig. 11 Microstructures of a solution annealed specimen which was previously soaked for 4.0 h

growth[34]. Several works have demonstrated the influence of precipitation on the ultrasonic nonlinearity parameter[32,34–36]. It is a fact that the nuclei of $M_{23}C_6$ precipitates can form in austenitic stainless steel during cooling cycle of the heat treatment if water quenching is delayed followed by solution annealing heat treatments. These precipitates grow continuously during soaking at 675 °C and get interconnected and get thicken. These carbide precipitates will act as a source of acoustic nonlinearity when they are excited by a high power ultrasonic wave. In order to confirm that the change in beta is because of the chromium carbide precipitation, the sensitized samples were subjected to solution annealing heat treatment at 1050 °C for 30 min and then analyzed by oxalic acid etching and second harmonic method. The relative β values for the specimens after solution annealing are plotted in Fig. 10. The relative β values remains almost close the non-sensitized base material.

It is clear that, the variation in relative beta with respect to the samples in the solution annealed condition is much less compared to that in the sensitized condition but it is not same as that of the base metal. Of course, ideally, the value of relative β parameter should have come down to that of the base metal, which is not sensitized. Slightly higher value of β with respect to that of the base metal could be due to other microstructural changes that have taken place in the material during the two additional heat treatments. The comparison of Fig. 3 with Fig. 11 shows that the grain size is increased in the solution annealed specimen. Further, there are some isolated grain boundaries which are still showing some sort of ditched structure even after the solution annealing. These factors could be the reasons for different relative beta values. However, substantial reduction in the relative beta value from the sensitized condition indicts that the de-sensitization is also can be detected by non linear ultrasonics.

Correlation between the DOS values calculated in EPR test and the relative beta values observed in nonlinear testing has been calculated by the Pearson correlation coefficient method by the following formula

$$\rho_{x,y} = \frac{\mathrm{cov}(x,y)}{\sigma_x \sigma_y} \tag{17}$$

where, $\mathrm{cov}(x,y)$ is the covariance of the two variables (x corresponds to DOS and y corresponds to the relative β), σ_x and σ_y are the respective standard deviations. The coefficient was found to be 96% which is reasonably a good correlation considering the experimental uncertainties. One to one correlation be-

tween degree of sensitization evaluated with different conventional procedures specified in ASTM standards and the relative nonlinear parameter has been obtained. Hence, the present study clearly demonstrates the potential of using nonlinear ultrasonics as a non-destructive testing technique to study sensitization of the austenitic stainless steel.

5. Conclusions

AISI Type 304 stainless steel has been subjected to different sensitization heat treatments. Degradation by sensitization has been studied by nonlinear ultrasonic techniques. It was found that relative β parameter increases with increase of soaking time which in turn due to increase in degree of sensitization. With 0.5, 1.0, 2.0, 3.0 and 4.0 h heat treatments at 675 °C, β increased by 15%, 40%, 56%, 62% and 63% respectively compared to that of the base material. One to one correlation between degree of sensitization evaluated with different conventional procedures specified in ASTM standards and the relative nonlinear parameter has been obtained. Hence the paper clearly demonstrates the potential of using nonlinear ultrasonics as a non-destructive testing technique to study sensitization of the austenitic stainless steel.

Acknowledgements

We thank our colleagues at Quality Assurance Division, Central Workshop Division, Physical Metallurgy Division and Corrosion Science and Technology Group at Indira Gandhi Centre for Atomic Research, Kalpakkam for their kind support and guidance during this work.

REFERENCES

[1] J.C. Lippold and D.J. Kotecki, Welding Metallurgy and Weldability of Stainless Steels, Wiley Interscience, 2005, p..
[2] F.R. Beckitt and B.R. Clark, Acta. Metall. **15** (1967) 113.
[3] M.H. Lewis and B. Hattersley, Acta. Metall. **13** (1965) 1159.
[4] E. Ranjbarnodeh, H. Pouraliakbar and A.H. Kokabi, Int. J. Mech. Appl. **2** (2012) 117.
[5] A.B. Korostelev, V.Y. Abramov and V.N. Belous, J. Nucl. Mater. **233–237** (1996) 1361.
[6] A.Y. Kina, V.M. Souza, S.S.M. Tavares, J.M. Pardal and J.A. Souza, Mater. Charact. **59** (2008) 651.
[7] V. Cihal and R. Stefec, Electrochim. Acta. **46** (2001) 3867.
[8] N. Parvathavarthini, R.K. Gupta, A.V. Kumar, S. Ramya and U.K. Mudali, Corros. Sci. **53** (2011) 3202.
[9] T.N. Prasanthi, C. Sudha, P. Parameswaran, R. Punniyamoorthy, S. Chandramouli, S. Saroja, K.K. Rajan and M. Vijayalakshmi, Eng. Fail. Anal. **31** (2013) 28.
[10] R.W. Fuller, J.Q. Ehrgott Jr., W.F. Heard, S.D. Robert, R.D. Stinson, K. Solanki and M.F. Horstemeyer, Eng. Fail. Anal. **15** (2008) 835.
[11] H. Shaikh, B.P.C. Rao, S. Gupta, R.P. George, S. Venugopal, B. Sasi, T. Jayakumar and H.S. Khatak, Brit. Corros. J. **37(2)** (2002) 129.
[12] H. Shaikh, N. Sivaibharasi, B. Sasi, T. Anita, R. Amirthalingam, B.P.C. Rao, T. Jayakumar, H.S. Khatak and B. Raj, Corros. Sci. **48** (2006) 1462.
[13] J. Stella, J. Cerezo and E. Rodriguez, NDT&E Int. **42** (2009) 267.
[14] J.H. Cantrell, Fundamentals and Applications of Nonlinear Ultrasonic Nondestructive Evaluation, In: T. Kundu, ed., Nondestructive Evaluation Engineering and Biological Material Characterization, CRC Press, New York, 2004, p. 363.
[15] D.C. Hurley, D. Balzar and P.T. Purtscher, J. Mater. Res. **15** (2000) 2036.
[16] A. Viswanath, B.P.C. Rao, S. Mahadevan, T. Jayakumar and B. Raj, J. Mater. Sci. **45** (2010) 6719.
[17] Y. Xiang, M. Deng, F.Z. Xuan and C.J. Liu, J. Appl. Phys. **111** (2012) 104905.
[18] A. Metya, M. Ghosh, N. Parida and S.P. Sagar, NDTE Int. **4** (2008) 484.
[19] K. Balasubramaniam, J.S. Valluri and R.V. Prasad, Mater. Charact. **62** (2011) 275.
[20] S. Baby, B.N. Kowmudi, C.M. Omprakash, D.V.V. Satyanarayana and K. Balasubramaniam, V. Kumar, Scr. Mater. **59** (2008) 818.
[21] A. Viswanath, B.P.C. Rao, S. Mahadevan, P. Parameswaran, T. Jayakumar and B. Raj, J. Mater. Proc. Technol. **211** (2011) 538.
[22] J.H. Cantrell and W.T. Yost, Int. J. Fatigue **23** (2001) 487.
[23] J.Y. Kim, L.J. Jacobs, J. Qu, J. Accoust. Soc. Am. **120** (2006) 1266.
[24] S.P. Sagar, S. Das, N. Parida and D.K. Bhattacharya, Scr. Mater. **55** (2006) 199.
[25] J.H. Cantrell, J. Appl. Phys. **106** (2009) 093516.
[26] A. Kumar, C.J. Torbet, J.W. Jones and T.M. Pollock, J. Appl. Phys. **106** (2009) 024904.
[27] V.V.S.J. Rao, E. Kannan, R.V. Prakash and K. Balasubramaniam, J. Appl. Phys. **104** (2008) 123508.
[28] H. Ogi, M. Hirao and S. Aoki, J. Appl. Phys. **90** (2001) 438.
[29] T.H. Lee and K.Y. Jhang, NDTE Int. **42** (2009) 757.
[30] K.H. Matlack, J.J. Wall, J.Y. Kim, J. Qu and L.J. Jacobs, J. Appl. Phys. **111** (2012) 054911.
[31] Y. Xiang, M. Deng, F.Z. Xuan and C.J. Liu, NDTE Int. **44** (2011) 768.
[32] C.S. Kim, I.K. Part and K.Y. Jhang, NDTE Int. **42** (2009) 204.
[33] S. Liu, A.J. Croxford, S.A. Neild and Z. Zhou, IEEE Trans. Ultrason. Ferroelectr. Freg. Control. **58** (2011) 1442.
[34] J.H. Cantrell and W.T. Yost, Appl. Phys. Lett. **77** (2000) 1952.
[35] J.H. Cantrell and W.T. Yost, J. Appl. Phys. **81** (1997) 2957.
[36] C. Mondal, A. Mukhopadhyay and R. Sarkar, J. Appl. Phys. **108** (2000) 124910.